COMPARISON OF TECHNIQUES FOR DAMAGE IDENTIFICATION BASED ON INFLUENCE LINE APPROACH

Ass. Prof. Dr. Eng. Štimac Grandić I.[1], Ass. Prof. Dr. Eng. Grandić D.[1], Prof. Dr. Eng.Bjelanović A.[1],
Faculty of Civil Engineering, University of Rijeka, Croatia [1]

Abstract: *Nondestructive damage identification is an important sub-problem of a damage assessment. In the paper the techniques for damage identification based on displacement influence lines and its derivatives for undamaged and damaged beam structure has been outlined. These techniques can be used for damage identification for both the simply supported and the continuous beams. The damage identification efficiency is investigated through techniques based on displacement influence lines is investigated. The numerical studies and experimental verification of the techniques have been carried out. The change in the rotation of displacement influence lines is generally the most reliable indicator for damage location.*

Keywords: DAMAGE IDENTIFICATION, DISPLACEMENT INFLUENCE LINE, BEAM STRUCTURES

1. Introduction

In the past few decades, non-destructive damage assessment has become increasingly important in order to determine safety and reliability of structures [1-5]. A great interest is shown in measurement optimization as well as in model optimization [6-11]. Generally, existing damage identification methods can be classified into two major categories: the dynamic and static identification methods. Both techniques are based on the correlation between two measured responses or comparison of the measured response to that obtained from an analytical or numerical model of the undamaged structure [1-11]. The main problem in many research papers arises from a limited number of measurement instruments [12-17]. This problem is overcome by using the influence line approach where one measurement point at each span is sufficient to conduct the damage assessment [18-20].

The approach presented in this paper is based on the changes in static response for the undamaged and damaged states of the structure due to changes in bending stiffness. In the paper, the damage identification efficiency using three different techniques based on displacement influence lines is investigated. The advantages and disadvantages for used damage identification techniques are outlined. The simplicity of presented techniques is mostly proved by the fact that a small number of measurement points in testing are required. Also a simple processing of measured data is applied to identify damage.

2. Damage identification techniques description

In a typical load-bearing structure, degradation of structural properties because of damage manifests itself as a change in static response.

Suppose we have two sets of the displacement influence lines for two states of the structure; the first state is undamaged and the second is damaged state. $\eta_w(x)=w(x)$ is the displacement influence line for the first state, $\overline{\eta_w}(x)=\overline{w}(x)$ is the displacement influence surface for the second state.

We assume that the system is geometrically and materially linear. Then, the rotation of displacement influence line and curvature of displacement influence line for both states can be written as

$$\varphi(x)=\frac{d(x)}{dx}, \qquad \overline{\varphi}(x)=\frac{d\overline{w}(x)}{dx} \tag{1}$$

$$\rho(x)=\frac{d^2w(x)}{dx^2}, \qquad \overline{\rho}(x)=\frac{d^2\overline{w}(x)}{dx^2} \tag{2}$$

The difference between the two states is represented by:

$$R(x)=\overline{w}(x)-w(x) \tag{3}$$

$$R_x(x)=\overline{\varphi}(x)-\varphi(x) \tag{4}$$

$$R_{xx}(x)=\overline{\rho}(x)-\rho(x) \tag{5}$$

Equation $R(x)\equiv 0$ shows that the two states of the structure are identical. When $R(x)\neq 0$, there is a change in the displacement influence line which points to changes in structural properties of the structure. In this case the first state can be assumed as undamaged state and the second state is damaged state of a structure. Also, the changes in rotation of the displacement influence lines and the changes in curvature of the displacement influence line for two structural states points to changes in structural properties.

The efficiency of following damage identification techniques will be investigated: change in the displacement influence lines $R(x)$, change in the rotation of displacement influence lines $R_x(x)$, change in the curvature of displacement influence lines, $R_{xx}(x)$.

3. Numerical studies

The analysis has been carried out for simply supported and continuous beams with different combination of damages. The span length of both beams is L=25 m. The cross section area of the beam is A=0.8567m2, the second moment of area is I=0.14 m4 and Young's modulus is E=3.5·107 kN/m2. The applied force is F=100 kN.

The displacement influence lines have been computed for point in the middle of each span for both the undamaged and the damaged state. The damage has been simulated by reducing the bending stiffness of some finite elements by 20%.

The displacement influence line is discrete function. Number and position of discrete points of displacement influence line depends on number of different position of applied load (sampling points).

The rotation and the curvature of the displacement influence lines have been calculated using finite difference method.

3.1 Simple supported beam

A simple supported beam has been modelled according to characteristic from Chapter 3. Numerical model of the beam is divided in n=100 finite elements. The length of each finite element is Δl=0.25 m. The force has been applied in every finite element knot (the sampling interval is 0.25 m).

The displacement influence lines have been constructed for the measurement point in the middle of the span.

3.1.1 Single damage scenario

In the first damaged case (damaged model 1) the damage is positioned at the 20th finite element (between finite element knots 19 and 20) as it is shown in Figure 1. In the second damaged case (damaged model 2) the damage is positioned at the 30th finite element (between finite element knots 29 and 30) as it is shown in Figure 2. In the third damaged case (damaged model 3) the damage is positioned at the 50th finite element (between finite element knots 49 and 50) as it is shown in Figure 3.

In Figures 1 to 3 the damaged beam models are shown at the top of the figures. Under the models, at the same Figures the change in the displacement influence lines (CDIL), the change in the rotation of displacement influence lines (CRDIL), and the change in the curvature of displacement influence lines (CCDIL) between undamaged and damaged beam are shown.

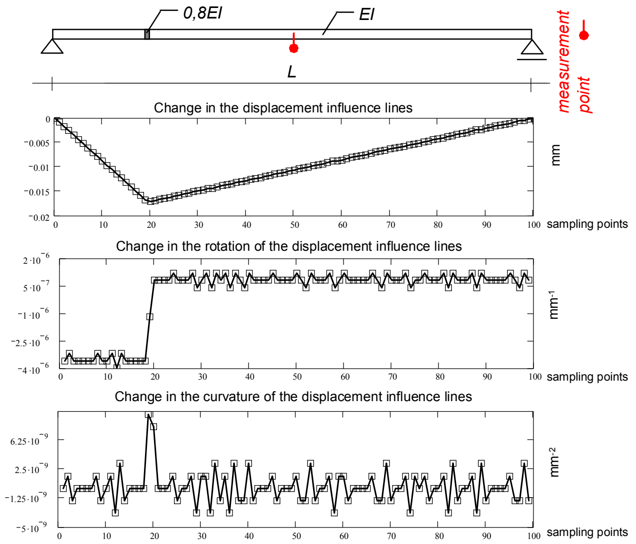

Fig. 1 *CDIL, CRDIL and CCDIL for damaged model 1*

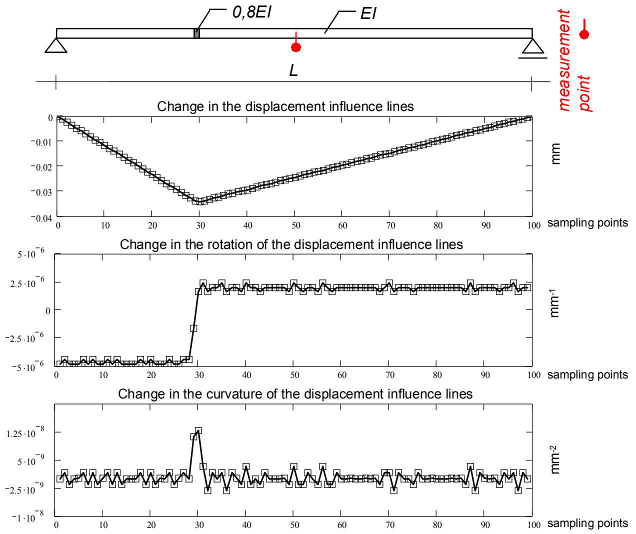

Fig. 2 *CDIL, CRDIL and CCDIL for damaged model 2*

From conducted analyses, it can be seen that all used damage identification techniques are able to identify the damage location (Figures 1 to 3). The change in the deflection influence lines for damaged and undamaged state have the maximum at the position of the damage. Also, position of damage is displayed with brake in the function of change in the deflection influence lines. The biggest values are calculated for the damage which is nearest to the measurement point (Figure 3) and the smallest for the furthest damage (Figure 1). The location of the damage is assessed by a vertical jump in the function of change in the rotation of the deflection influence lines. As in the previous case, the biggest value of vertical jump is calculated for the damage which is nearest to the measurement point and the smallest for the furthest damage (Figures 1 to 3).

The change in curvature of the deflection influence lines shows the peak at the location of the damage. In this case, also as in the previous two cases, the biggest value of the peak is calculated for the damage which is nearest to the measurement point and the smallest for the furthest damage (Figures 1 to 3). From conducted analyses it can be concluded that the damage near to the measurement point will be detected with more accuracy than the damage which is located far from the measurement point.

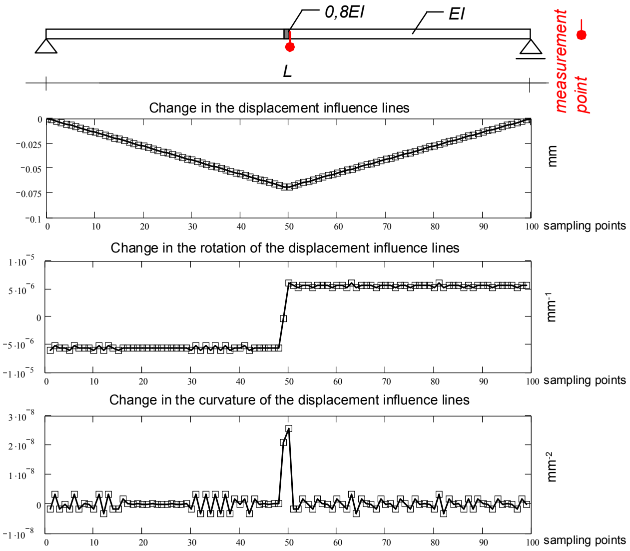

Fig. 3 *CDIL, CRDIL and CCDIL for damaged model 3*

3.1.1 Multiple damage scenario

In the fourth case (damaged model 4 in Figure 4) the two damages are positioned at the 20th finite element and at the 30th finite element (between finite element knots 19 and 20 and between 29 and 30) and in fifth case (damaged model 5 in Figure 5) the two damages are positioned at the 20th finite element and at the 70th finite element (between finite element knots 19 and 20 and between 69 and 70).

As it can be seen from Figures 4 and 5 the change in the deflection influence lines for the damaged an the undamaged state are not reliable indicator if there are more then one damage (especially when damages are close to one another as it is in the damaged model 4).

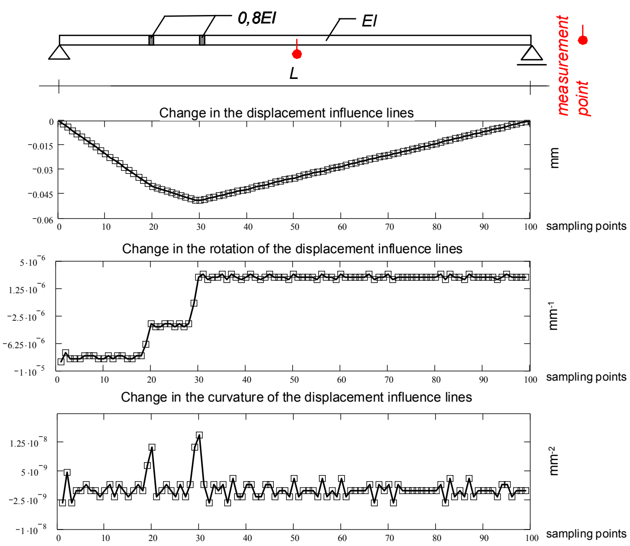

Fig. 4 *CDIL, CRDIL and CCDIL for damaged model 4*

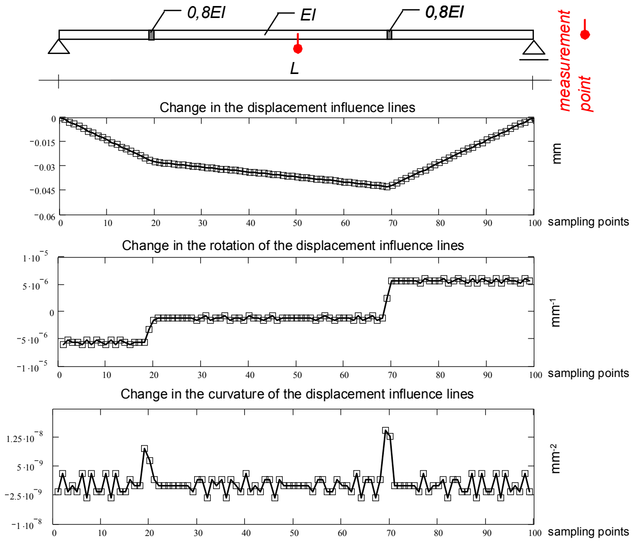

Fig.5 *CDIL, CRDIL and CCDIL for damaged model 5*

3.2 Continuous beam

A two-span continuous beam has been modelled according to characteristics from Chapter 3. Numerical model of the beam is divided in n=100 finite elements. The length of each finite element is Δl=0,25 m. The force has been applied in every finite element knot (the sampling interval is 0,5 m). The displacement influence lines have been constructed for two measurement point in the structure; in the middle of the first span and in the middle of the second span. The analyses of the displacement influence lines have been conducted for both measurement points.

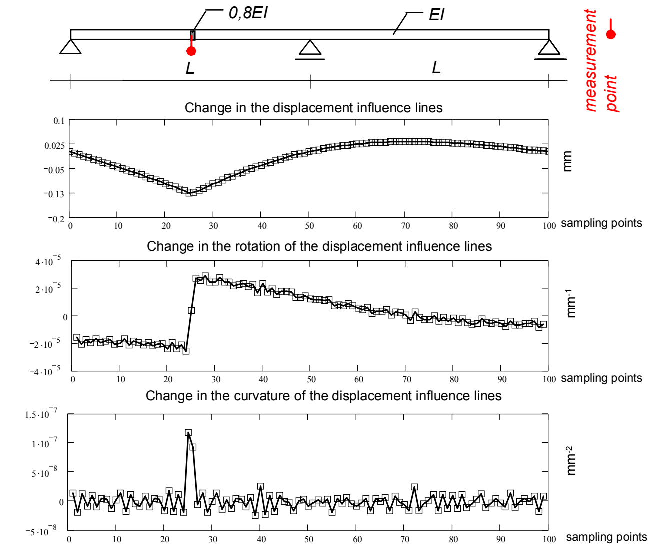

Fig.6 *CDIL, CRDIL and CCDIL for damaged model 6 (measurement in the first span)*

In the sixth damaged case (damage model 6) the damage is positioned at the 26th finite element in the first span (between finite element knots 25 and 26) as it is shown in Figures 6 and 7. In the seventh case (damaged model 7 in Figures 7 and 8) the two damages are positioned at the 26th finite element in the first span and at the 90th finite element in the second span (between finite element knots 25 and 26 and between 89 and 90).

As it can be seen from Figures 6 to 9 the changes in the deflection influence lines are not always reliable to damage assessment if the damage is located in one span and the measurement point is in the other span (Figure 7). Also the change in the rotation of the deflection influence lines and change in the curvature of the deflection influence lines detect reliably only the damages which is positioned in the same span as the measurement point (Figures 6 and 7).

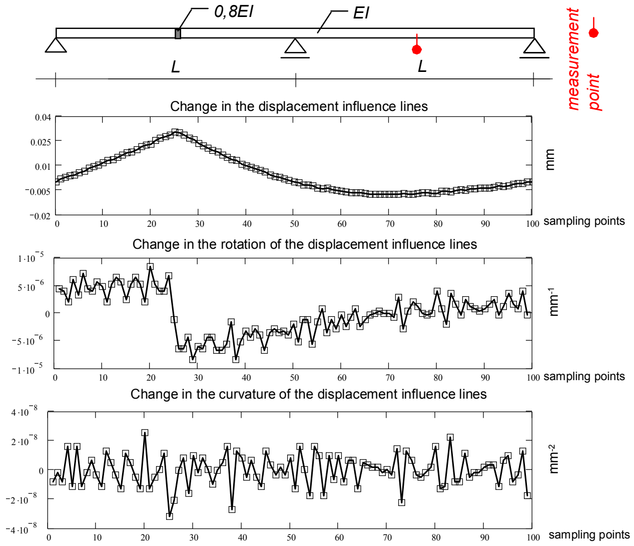

Fig.7 *CDIL, CRDIL and CCDIL for damaged model 6 (measurement in the second span)*

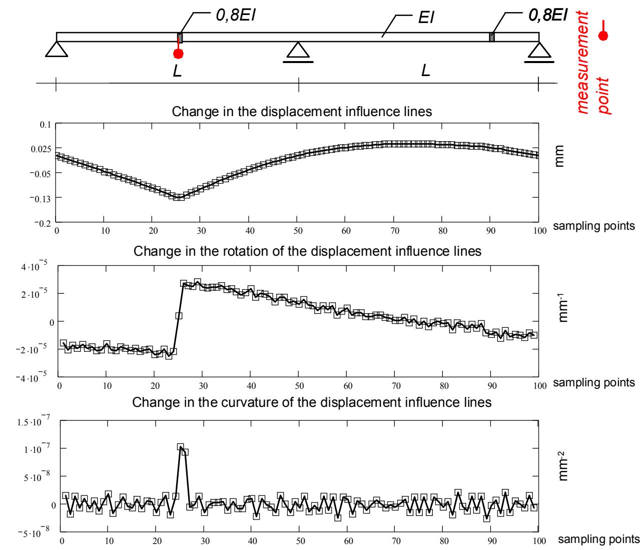

Fig.8 *CDIL, CRDIL and CCDIL for damaged model 7 (measurement in the first span)*

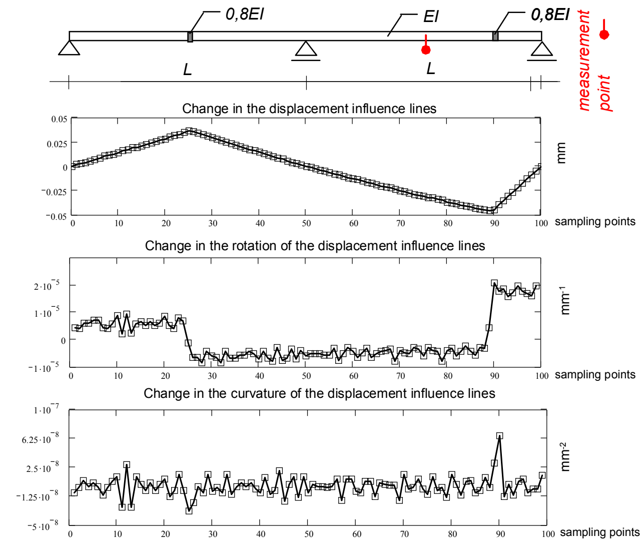

Fig.9 *CDIL, CRDIL and CCDIL for damaged model 7 (measurement in the second span)*

3.3 Sampling modification

In this chapter, the influence of number of sampling points will be investigated. Reduction of sampling points has been done in analyzing the fifth damaged model from Chapter 3.1.2. In the Figure 10 results of damage identification techniques using deflection influence lines with twice the smaller number of sampling points than in chapter 3.1.2 are shown (the sampling interval is 0,5 m) .

In Figures 1 and 12 the results of damage detection techniques by using five times and ten times smaller number of sampling points than in chapter 3.1.2 respectively are shown. The sampling interval is 1,25 m for analyses conducted and showed Figure 11 and 2 m for analyses conducted and showed on the right side of Figure 12.

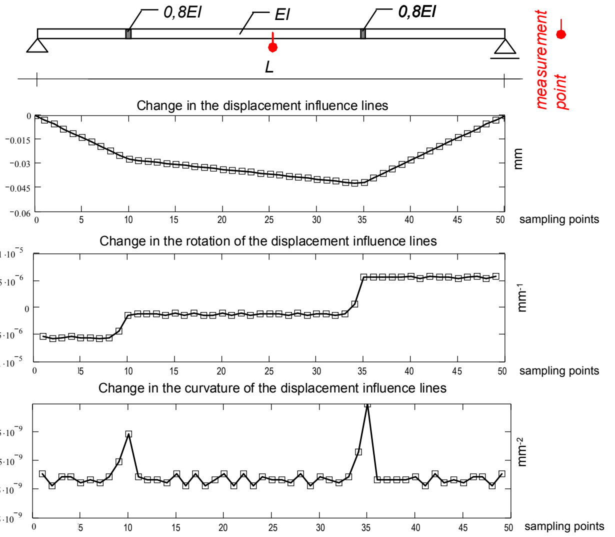

***Fig10** CDIL, CRDIL and CCDIL for damaged model 5; the sampling interval 0,5 m*

As it can be seen from Figures 10 to 12, the damage identification is successful regardless of number of sampling points. The smallest number of sampling points gives the roughest identification. It shows that application of this method can be successful even with small number of sampling points. When the potential location of damage is found by using small number of sampling points the potential damaged location can be tested again with smaller sampling interval to determine the damage location more accurately.

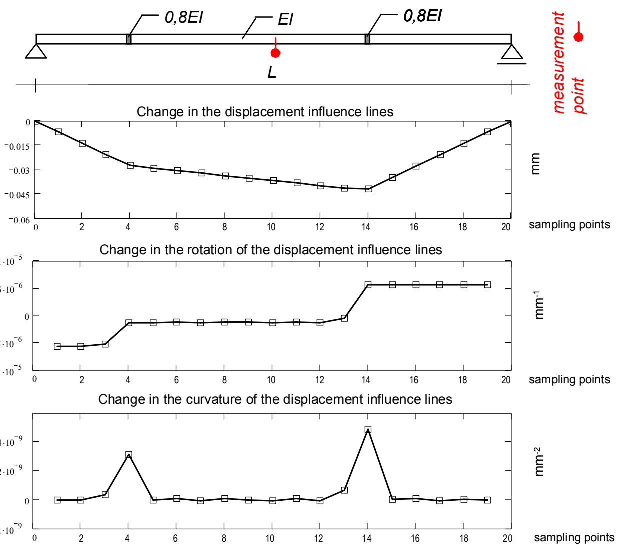

***Fig.11** CDIL, CRDIL and CCDIL for damaged model 5; the sampling interval 1,25 m*

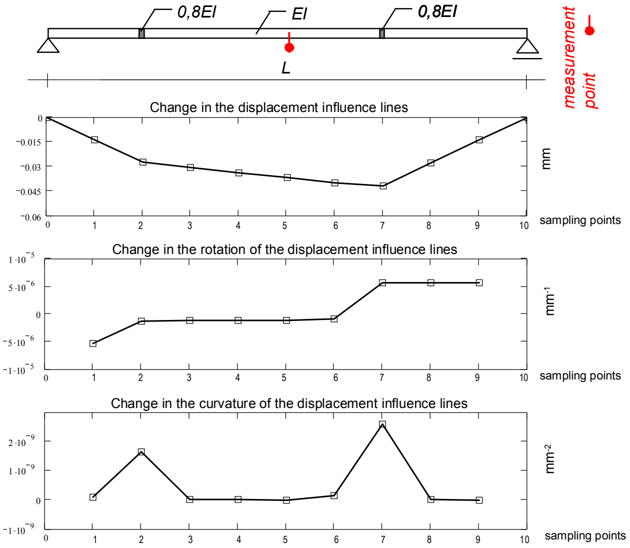

***Fig.12** CDIL, CRDIL and CCDIL for damaged model 5; the sampling interval 2,5 m*

4. Experimental verification

Experimental validation is done by using on-site testing measurements (Figure 13). On-site testing is carried out on the beam specimen shown in Figures 14 and 15. The span length of the specimen is L=6 m. The beam specimen had six longitudinal reinforcing bars embedded in the concrete (4ϕ7 mm and 2ϕ8 mm) in the low part of specimen and two longitudinal bars (2ϕ8 mm) at the top of the specimen. The longitudinal bars of the low and top part of specimen were connected together by mesh of bars of ϕ4.2 mm. At the position of 1.6 to 1.8 meters from left support two of ϕ8 mm bars in the low part of specimen were cut off.

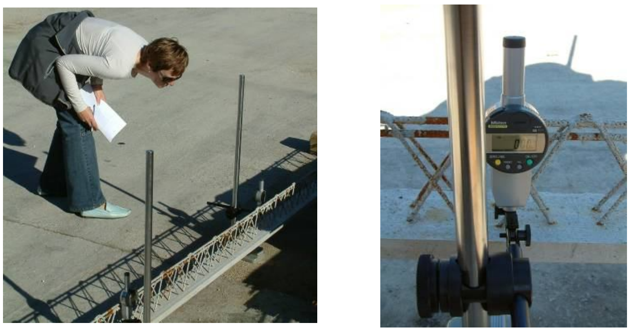

Fig. 13 On-site testing

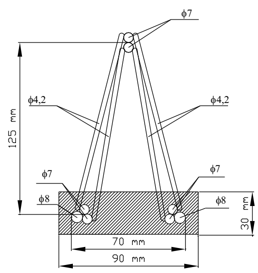

Fig.14 The cross-section of the specimen

The deflections were measured by digital indicator (Figure 13) in the middle of the span. The load was applied successively every 40 cm starting from the left support. The applied force was 0.28 kN. The obtained displacements values in the middle of the span are used to construct the deflection influence line of the damaged specimen. The deflection influence line in the middle of the span for the undamaged specimen was calculated by using idealized stiffness of undamaged cross-section.

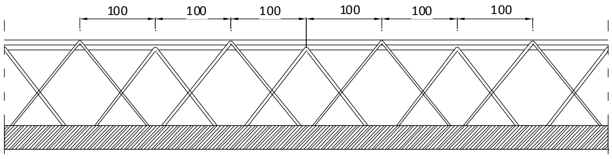

Fig.15 The detail of the longitudinal view of specimen

In Figure 16 the specimen model and damage identification techniques based deflection influence lines are show.

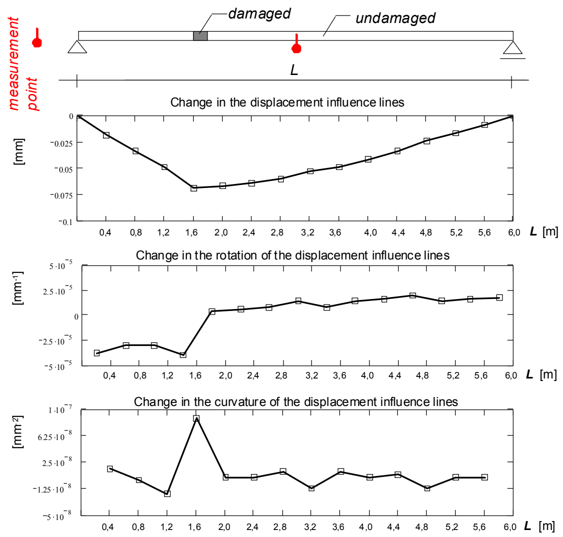

Fig.16 *CDIL, CRDIL and CCDIL for damaged specimen*

All of three damage identification techniques are able to detect the damage (Figure 16). Change in the displacement influence lines point to position of 1.6 m as well as the change in curvature of the displacement influence lines. The change in rotation of the displacement influence lines localized damage segment between 1.4 and 1.8 m. According to real position of the damage (between 1.6 and 1.8 meters), it can be concluded that developed damage identification techniques based on displacement influence lines can be successfully applied to detect and locate the real damage.

5. Conclusion

According to conducted numerical studies and experimental verification developed damage identification techniques based on displacement influence lines can be successfully applied to detect and locate the damage.

If single damage is located in the same span as the measurement point all three techniques can successfully locate the damage. If there is more then one damage the change in displacement influence line will detect only the damage which is nearer to the measurement point. Change in rotation and curvature of the displacement influence lines can locate multiple damages in simple supported beams but for continuous beams only damages located in the same span as the measurement point be detect without doubt. That points that the measurement point is necessary in every span. Sometimes, the change in curvature displacement influence line can give some misleading indicators of damages due to numerical inaccuracy of the finite difference method. Generally, the change in rotation of the displacement influence line shows the most reliable results in damage localization.

Presented techniques are simple for the conduct of on-site measurements because one measurement point in the middle of each span enables locating the damages reliably even with small number of sampling points.

6. References

[1] Hajela P., Soeiro F.J., Structural damage detection based on static and modal analysis, AIAA Journal, 28(6), p. 1110–1115, 1989.
[2] Doebling S.W., Farrar C.R., Prime M.B., Shevitz S.W., Damage identification and health monitoring of structural and mechanical systems from changes in their vibration characteristics: a literature review, National Laboratory Report LA-13070-VA5, Los Alamos, 1996.
[3] Zou Y., Tong L., Steven G.P., Vibration-based model-dependent damage (delamination) identification and health monitoring for composite structures—a review, Journal of Sound and Vibration, 30, p. 357–78, 2000
[4] Doebling S.W., Farrar C.R., Prime M.B., A summary review of vibration-based damage identification methods, The Shock and Vibration Digest, 30(2), p. 91–105, 1998.
[5] Li ,Y.Y., Hypersensitivity of strain-based indicators for structural damage identification: A review, Mechanical Systems and Signal Processing, 24, p. 653–664, 2010.
[6] Li Y.Y., Yam L.H., Sensitivity analyses of sensor locations for vibration control and damage detection of thin-plate systems, Journal of Sound and Vibration, 240(4), p. 623–636, 2001.
[7] Yam L.H., Li Y.Y., Wong W.O., Sensitivity studies of parameters for damage detection of plate-like structures using static and dynamic approaches, Engineering Structures, 24(11), p. 1465-1475, 2002.
[8] Sazonov E., Klinkhachorn P., Optimal spatial sampling interval for damage detection by curvature or strain energy mode shapes, Journal of Sound and Vibration, 285(4-5), 783-801, 2005.
[9] Choi F.C., Li J., Samali B., Crews K., Application of the modified damage index method to timber beams, Engineering structures, 30(4), p. 1124-1145, 2008.
[10]Huiwen, W. Chengbo, Development of scanning damage index for the damage detection of plate structures using modal strain energy method, Mechanical Systems and Signal Processing, 23(2), p. 274-287, 2009.
[11] N. Stubbs, J.-T. Kim, K. Topole, An efficient and robust algorithm for damage localization in offshore platforms, in Proceedings of the ASCE Tenth Structures Congress, San Antonio, p. 543-546, 1992.
[12] P. Cornwell, S.W. Doebling, C.R. Farrar, Application of the strain energy damage detection method to plate-like structures, Journal of Sound and Vibration, 224(2), p. 359–374, 1999.
[13] H. Huiwen, W. Bor-Tsuen, L. Cheng-Hsin, S. Jing-Shiang, Damage detection of surface cracks in composite laminates using modal analysis and strain energy method, Composite Structures, 74(4), p. 399-405, 2006.
[14] W.L. Bayissa, N. Haritos, Structural damage identification in plates using spectral strain energy analysis, Journal of Sound and Vibration, 307(1-2), p. 226-249, 2007.
[15] F.C. Choi, J. Li, B. Samali, K. Crews, Application of the modified damage index method to timber beams, Engineering structures, 30(4), p. 1124-1145, 2008.
[16] M. Kumar, R.A. Shenoi, S.J. Cox, Experimental validation of modal strain energies based damage identification method for a composite sandwich beam, Composite Science and Technology, 69(10), p. 1635-1643, 2009.
[17] Owolabi, G. M., Swamidas, A. S. J., Seshadri, R., Crack detection in beams using changes in frequencies and amplitudes of frequency response function, Journal of Sound and vibration, Vol. 265, p. 1-22, 2003.
[18] I. Stimac, I. Kozar, A. Mihanovic, Beam damage detection by deflection influence lines, Gradevinar, 59(12), p. 1053-1066, 2007.
[19] C.Y. Wang, C.K. Huang, Y. T. Zeng, C. S. Chen, M. H. Chen, Damage Assessment of Beam by a Quasi-Static Moving Vehicular Load, Proceedings of 10th International Conference on Structural Safety and Reliability, Osaka, Japan, p. 803-809, 2009.
[20] I.Y. Choi, J. S. Lee, E. Choi, H.N. Cho, Development of elastic damage load theorem for damage detection in statically determinate beam, Computers and structures, 82(29-30), p. 2483-2492, 2004.